

1 **Osmium isotopes in Baffin Island and West Greenland picrites:**
2 **Implications for the $^{187}\text{Os}/^{188}\text{Os}$ composition of the convecting mantle**
3 **and the nature of high $^3\text{He}/^4\text{He}$ mantle**

4 C.W. Dale^{a*}, D.G. Pearson^a, N.A. Starkey^{b,c}, F.M. Stuart^b, L.M. Larsen^d, R.M.
5 Ellam^b, J.G. Fitton^c, C.G. Macpherson^a

6 *^aDepartment of Earth Sciences, Durham University, Science Laboratories, Durham, DH1 3LE, UK*

7 *^bIsotope Geosciences Unit, SUERC, East Kilbride, G75 0QF, UK*

8 *^cSchool of GeoSciences, University of Edinburgh, Edinburgh, EH9 3JW, UK*

9 *^dGeological Survey of Denmark & Greenland, Ostervoldgade 10 DK, 1350 Copenhagen, Denmark*

10 *corresponding author. email: christopher.dale@durham.ac.uk. Tel: +44 0191 3342338,

11 Fax: +44 0191 3342301

12

13 **Abstract**

14 Identifying the Os isotope composition of the prevalent peridotitic convecting mantle places
15 important constraints on the Earth's accretion, differentiation and evolution and also has
16 implications for the interpretation of Re-depletion ages in mantle peridotites. As partial melting
17 preferentially samples components with the lowest melting temperatures, large degree melts such as
18 picrites should most closely reflect the peridotitic components within the source. Thus, Re-Os
19 analyses of thirty picrites from Baffin Island and West Greenland are thought to provide a good
20 estimate of the bulk $^{187}\text{Os}/^{188}\text{Os}$ composition of their convecting mantle source, which is
21 indistinguishable from DMM in terms of lithophile isotopes and trace elements. In addition, the
22 high $^3\text{He}/^4\text{He}$ of these rocks allows us to comment on the possible origins of high $^3\text{He}/^4\text{He}$ mantle.
23 Ingrowth-corrected $^{187}\text{Os}/^{188}\text{Os}$ of the picrites ranges from 0.1267 to 0.1322. The higher $^{187}\text{Os}/^{188}\text{Os}$
24 samples have correspondingly lower $^{143}\text{Nd}/^{144}\text{Nd}$ which may reflect a contribution (~5%) from old
25 recycled oceanic crust, including sediment. However, Baffin Island and the earliest West
26 Greenland picrites are remarkably uniform in composition with $^{187}\text{Os}/^{188}\text{Os}$ between 0.1267 and
27 0.1280, and a mean and mode of 0.1272 ± 0.0007 . Such Os isotope compositions are less
28 radiogenic than estimates of primitive upper mantle but are similar to the least radiogenic mid-
29 ocean ridge basalts (MORB) and the most common composition of ophiolite-derived platinum-
30 group alloys and chromites. These compositions appear to represent a source dominated by
31 peridotite.

32 The picrites studied record the highest known $^3\text{He}/^4\text{He}$ in the silicate Earth (up to $50 R_a$). For this
33 signature to reflect isolated domains of ancient melt depletion would require significantly less
34 radiogenic Os isotope compositions than observed ($^{187}\text{Os}/^{188}\text{Os}$: <0.115), unless radiogenic Os, but
35 not He, has been subsequently added. Conversely, a bulk outer core contribution would impart a
36 supra-chondritic $^{187}\text{Os}/^{188}\text{Os}$ signature to the picrites, and thus Os isotopes preclude the core as a

37 source of high $^3\text{He}/^4\text{He}$, unless core-mantle transfer of Os and He is decoupled. It is possible to
38 broadly account for the Os-He and Os-Nd isotope variations by mixing of depleted MORB mantle,
39 recycled oceanic crust and primitive mantle with high $^3\text{He}/^4\text{He}$, but it is difficult to explain each
40 individual sample composition in this way. Alternatively, as the high $^3\text{He}/^4\text{He}$ signature is found in
41 samples with variable Os and Nd isotope compositions, it seems likely that He is decoupled from
42 other isotopic tracers and is dominated by minor addition of a He-rich, high $^3\text{He}/^4\text{He}$ component
43 probably of primordial nature, although the ultimate source is unclear from our data.

44 Keywords: osmium isotopes, helium isotopes, Baffin Island, West Greenland, picrite, convecting
45 mantle, depleted mantle.

46 **1. Introduction**

47 Mantle rocks and mantle-derived melts display a broad range of Os isotope compositions, both
48 depleted and enriched with respect to bulk Earth and primitive upper mantle (PUM) estimates. Due
49 to the differential compatibility of Re and Os during mantle melting, crustal rocks typically have
50 very high Re/Os ratios and, over time, evolve to radiogenic $^{187}\text{Os}/^{188}\text{Os}$ compared to the mantle.
51 Depleted mantle evolves complementary unradiogenic $^{187}\text{Os}/^{188}\text{Os}$ ratios, with the timing of Re
52 depletion indicated by the extent to which $^{187}\text{Os}/^{188}\text{Os}$ deviates below a chondritic evolution curve.
53 Therefore, the Re-Os system is a powerful tool with which to assess contributions from depleted
54 mantle and enriched recycled materials to the source of mantle-derived melts (e.g. Shirey and
55 Walker, 1998).

56 Significant Os isotope heterogeneity exists in the mantle at a variety of length-scales from mineral-
57 to vein- to slab-scale due to the recycling of enriched crustal materials and depletion of peridotite,
58 and due to the highly siderophile nature of both Re and Os. Variable degrees of melting of such a
59 heterogeneous mantle will lead to melts that vary in isotopic composition, where melts with the

60 most radiogenic signature are typically derived from the smallest degrees of melting, and large-
61 degree melts give the best estimate of the $^{187}\text{Os}/^{188}\text{Os}$ composition of the *bulk* mantle source. This
62 study of North Atlantic (NA) picrites from Baffin Island (BI) and West Greenland (WG) should
63 therefore provide a good estimate for the average Os isotope composition of the whole source
64 volume. Given the lithophile isotope similarity of this source to depleted mid-ocean ridge basalt
65 (MORB) mantle (DMM, e.g. Ellam and Stuart, 2004), this signature should also provide an estimate
66 for the $^{187}\text{Os}/^{188}\text{Os}$ of typical convecting mantle without significant contribution from enriched
67 components. Such an estimate is a valuable addition to current constraints on the Os isotope
68 evolution of the Earth and peridotite melting ages (e.g. Meisel et al., 2001; Walker et al., 2002b).

69 The Baffin Island and West Greenland picrites define the high $^3\text{He}/^4\text{He}$ end-member of the mantle
70 range (up to 50 R_a , Stuart et al., 2003; Starkey et al., 2008, in press), which includes the canonical
71 MORB range of $8 \pm 1 R_a$ (Graham, 2003; where $R_a = ^3\text{He}/^4\text{He}_{\text{atmosphere}} = 1.39 \times 10^{-6}$). The picrites
72 were erupted at about 61 Ma, probably due to the onset of the proto-Iceland plume (Saunders et al.,
73 1997), and this melting region continues to produce mantle melts with high $^3\text{He}/^4\text{He}$ in the Iceland
74 region today (Macpherson et al., 2005). Due to the incompatibility of He, conventional wisdom
75 posits that high $^3\text{He}/^4\text{He}$ mantle reservoirs are less degassed than the convecting upper mantle, and
76 retain a component of the Earth's primordial volatile inventory (e.g. Kurz et al., 1982; Moreira et
77 al., 2001; Porcelli et al., 2002). However, the observation that U and Th may be less compatible
78 than He in an olivine-rich mantle assemblage has led to the suggestion that high $^3\text{He}/^4\text{He}$ may result
79 from the greater loss of U and Th than He during ancient melt depletion (Graham et al., 1990; Class
80 and Goldstein, 2005; Parman et al., 2005). The Re-Os isotope system has the ability to retain
81 information about mantle melting events, even in the convecting mantle (e.g. Brandon et al., 2000;
82 Meibom et al., 2002; Harvey et al., 2006; Pearson et al., 2007), and thus is the most suitable tracer
83 to test whether high $^3\text{He}/^4\text{He}$ signatures can be directly linked to ancient depletion events.

84 In this study, Os isotope data for North Atlantic picrites from Baffin Island and West Greenland
85 have been (i) used to gain an estimate of the average $^{187}\text{Os}/^{188}\text{Os}$ composition of the convecting
86 mantle, and (ii) combined with existing He and Nd isotope data to re-assess the nature of the highest
87 known $^3\text{He}/^4\text{He}$ mantle component.

88 **2. Samples: setting and chemistry**

89 The picrites in this study were collected from the eastern margin of Baffin Island (BI) at Cape
90 Searle, Padloping Island and Durban Island and from Disko Island (Qeqertarsuaq) and the
91 Nuussuaq peninsula in West Greenland (WG). The WG picrites were collected from the three
92 members of the Vaigat formation, from oldest to youngest, the Anaanaa, Naujánguit and
93 Ordlingassoq Members. Sampling focussed on olivine-rich samples, but is otherwise representative
94 of the units sampled. The BI picrites are undifferentiated stratigraphically, but can be grouped
95 chemically into the enriched (E-type) lavas (DUR-8, DI-23 and PAD-6) and normal (N-type) lavas
96 (all others) first identified by Francis (1985). Sample CS-7 is from a cross-cutting dyke, and not
97 from the picrite lava succession. Volcanism was largely contemporaneous on Baffin Island and in
98 West Greenland and commenced ~61 Ma (Storey et al., 1998). Picrites from BI and the Anaanaa
99 and lower Naujánguit Members of WG possess normal magnetisation whereas the subsequent WG
100 melts are reversely magnetised (Pedersen et al., 2002). All members, and ~80% of the entire
101 Paleocene volcanic sequence, were erupted within 1 million years (Storey et al., 1998).
102 Petrography, major and trace element chemistry and Sr, Nd and Pb isotopes are described in more
103 detail in previous studies (e.g. Francis, 1985; Holm et al., 1993; Graham et al., 1998; Larsen and
104 Pedersen, 2000; Kent et al., 2004).

105 All North Atlantic (NA) picrites have high MgO contents compared to most mantle melts (up to 27
106 wt. % in this study) which, although in part a result of olivine accumulation, reflects the Mg-rich
107 nature of parental melts. Estimates for the parental melts of WG picrites, based on Fo-rich olivine

108 phenocrysts, vary between 18 and 21 wt. % MgO (Pedersen, 1985; Larsen and Pedersen, 2000;
109 Herzberg and O'Hara, 2002). Such MgO contents indicate generation by a high degree of melting -
110 10-11% for a depleted source (Herzberg and O'Hara, 2002; twice as high as MORB melting) - of
111 anomalously hot mantle (1540-1600°C) at depths of 60-90 km (Pedersen, 1985; Gill et al., 1992;
112 Herzberg and O'Hara, 2002). The high degree of melting generates Os-rich melts which are less
113 susceptible to interactions with crust and lithospheric mantle – critical when looking at samples
114 erupted through ancient continental crust and lithosphere.

115 The three West Greenland picrite members have similar major element characteristics. However,
116 for a given MgO content, TiO₂ increases with time, possibly reflecting a changing contribution from
117 enriched material in the picrite source (cf. Prytulak and Elliott, 2007), with the older WG picrites
118 most closely resembling the Baffin picrites (Holm et al., 1993). Chondrite-normalised REE patterns
119 are flattest in the Anaanaa and Naujánguit picrites, while the Ordlingassoq samples have higher
120 LREE and incompatible element concentrations (Holm et al., 1993). Neodymium and Sr isotope
121 compositions of the Ordlingassoq picrites resemble the least depleted Iceland picrites (Holm et al.,
122 1993).

123 **3. Analytical techniques**

124 Approximately 1g of each whole rock powder was digested and equilibrated with a mixed ¹⁹⁰Os–
125 ¹⁸⁵Re-enriched spike, using inverse aqua regia (2.5 mL 12 mol L⁻¹ HCl and 5 mL 16 mol L⁻¹ HNO₃)
126 in a quartz high-pressure asher (HPA) vessel or borosilicate Carius tube. HPA vessels were placed
127 in an Anton-Paar HPA at Durham University at 300°C and >110 bars for at least 12 hours, and
128 Carius tubes were placed in an oven at 240°C for at least 36 hours. Osmium was extracted using
129 CCl₄, back-extracted using HBr, and then microdistilled (Cohen and Waters, 1996). The aqua regia
130 was dried, re-dissolved in 0.5 mol L⁻¹ HCl, and Re was separated using AG1X-8 (100-200#) anion-
131 exchange resin (Pearson and Woodland, 2000).

132 Osmium was loaded onto Pt filaments and measured as OsO_3^- ions by negative-thermal ionisation
133 mass spectrometry (N-TIMS) using the ThermoFinnigan Triton at Durham University. All Os
134 isotope beams and mass 233, corresponding to $^{185}\text{ReO}_3^-$, were measured sequentially using an axial
135 secondary electron multiplier. Raw data were corrected offline for O isotope interference, mass
136 fractionation (using $^{192}\text{Os}/^{188}\text{Os} = 3.08271$) and spike unmixing. Interference from $^{187}\text{ReO}_3^-$ was
137 insignificant (<2 cps). Analyses of 170 pg aliquots of the University of Maryland Os standard
138 solution (UMd, or UMCP) gave mean $^{187}\text{Os}/^{188}\text{Os}$ of 0.11384 ± 16 (2σ , $n=19$) and 0.11379 ± 14 (2σ ,
139 $n=39$) for the two periods of analysis, April - November 2002 and April - May 2008, respectively.
140 These values are in good agreement with a value of 0.113787 ± 7 for 10-100 ng/g aliquots measured
141 on the same mass spectrometer in Faraday cup mode (Luguet et al., 2008a). Rhenium was analysed
142 by inductively-coupled plasma mass spectrometry (ICP-MS) on a ThermoFinnigan[®] Element 2.
143 Solutions were introduced using a micro-concentric nebuliser and a dual-cyclonic quartz spray
144 chamber. A standard Re solution (1 ng/g) was analysed at the start, middle and end of each session
145 to determine mass fractionation.

146 Carius tube and HPA digestions gave, respectively, mean total procedural blanks of 0.43 and 0.32
147 pg Os, 2.5 and 1.9 pg Re, and $^{187}\text{Os}/^{188}\text{Os}$ of 0.143 and 0.192. Blank corrections relate to the
148 appropriate reagent batch rather than a long-term mean, but were always less than 0.1% for
149 concentration and isotope composition.

150 *Reproducibility of samples.* Duplicate digestions of an Os-rich (~2 ng/g) and Os-poor sample (~0.5
151 ng/g) indicate $^{187}\text{Os}/^{188}\text{Os}$ reproducibility of 0.15% and 0.7% (2 RSD, $n=3$), respectively (Table 1).
152 Os concentrations are reproducible to ~5% and 11% (2 RSD) for the two samples, respectively, and
153 Re concentrations ($n=2$) vary by less than 1% (2 RSD) for both samples. The external accuracy of
154 analyses is more difficult to evaluate, but reproducibility using two different digestion techniques
155 for these samples and for reference materials (Dale et al., 2008; Dale et al., 2008, in press) suggests

156 that incomplete digestion and/or sample-spike equilibration is unlikely to be a significant
157 consideration.

158 **4. Results**

159 **4.1 Re and Os elemental data**

160 Osmium concentrations range from 1.50 to 4.02 ng/g in the West Greenland picrites and from 0.435
161 to 3.45 ng/g in the Baffin Island picrites (Table 1). The WG suite has a higher median of 2.49 ng/g
162 Os compared to 1.66 ng/g for the Baffin suite. All samples have much greater Os concentrations
163 than MORB, which range from <0.001 to 0.25 ng/g (Roy-Barman and Allegre, 1994; Gannoun et
164 al., 2007). The highest Os concentrations are greater than approximate averages for primitive or
165 depleted mantle (~3.1-3.7 ng/g, Morgan et al., 2001; Becker et al., 2006; Harvey et al., 2006).
166 Rhenium concentrations vary from 0.113 to 0.506 ng/g in the BI picrites, with a median of 0.32
167 ng/g, while the WG samples have a larger range (0.063 to 1.14 ng/g) but a similar median of 0.29
168 ng/g. Such Re abundances are typically lower than MORB (0.34 – 2.28 ng/g, median ~1 ng/g, Sun
169 et al., 2003; Gannoun et al., 2007).

170 Figure 1 here.

171 Osmium concentrations decrease with decreasing MgO (Figure 1) and Ni (not shown). For a given
172 MgO content, WG picrites tend to be more Os-rich than BI picrites, which are both richer in Os
173 than recent Iceland picrites (Brandon et al., 2007). Co-variation of MgO and Re is less systematic
174 than with Os, but a negative co-variation exists in the BI samples and is well-defined in two
175 regional sub-sets (see Figure 1). With the exception of several samples, Re/Os ratios increase with
176 decreasing MgO content in all suites (compare Figure 1a & b).

177 Table 1 here.

178 4.2 Os isotope data

179 Baffin Island picrites have a range of $^{187}\text{Os}/^{188}\text{Os}$ from 0.1269 to 0.1344, which, when corrected for
180 ingrowth of ^{187}Os since the time of emplacement (61 Ma), gives a narrow range of initial
181 $^{187}\text{Os}/^{188}\text{Os}$ ratios from 0.1267 to 0.1287. The most radiogenic picrite has the lowest Os
182 concentration (~ 0.45 ng/g, Figure 3), consistent with a previous conclusion of crustal contamination
183 for this sample (Stuart et al., 2003); this sample has been excluded from further discussion. Thus,
184 the range of initial $^{187}\text{Os}/^{188}\text{Os}$ is considerably more limited, from 0.1267 to 0.1278. The WG
185 picrites have a larger range of $^{187}\text{Os}/^{188}\text{Os}$ and $^{187}\text{Os}/^{188}\text{Os}_{\text{initial}}$ of 0.1271 – 0.1332 and 0.1267 -
186 0.1322, respectively. However, the least radiogenic WG samples form a peak on an initial
187 $^{187}\text{Os}/^{188}\text{Os}$ probability density plot at 0.1272, which is identical to the BI peak (Figure 2). The sub-
188 chondritic to supra-chondritic range of Os isotope values observed in a different suite of BI picrites
189 (Kent et al., 2004) was not found in this study. Source heterogeneity is a possible explanation for
190 this difference but as the samples of Kent et al. (2004) have unusually high Os concentrations for
191 their MgO content (Figure 1), and Os co-varies with $^{187}\text{Os}/^{188}\text{Os}$, we contend that these samples
192 may have been modified during interaction with an Os-rich, low $^{187}\text{Os}/^{188}\text{Os}$ lithospheric mantle
193 component (cf. Larsen et al., 2003).

194 The WG picrites extend to more radiogenic Os isotope compositions than the BI picrites, and
195 $^{187}\text{Os}/^{188}\text{Os}$ clearly varies with stratigraphy. Picrites from the Anaanaa and Naujáunguit Members of
196 the Vaigat formation possess largely uniform and unradiogenic $^{187}\text{Os}/^{188}\text{Os}$ (Figure 3). In contrast,
197 all samples from the slightly younger Ordlingassoq Member have more radiogenic $^{187}\text{Os}/^{188}\text{Os}_{\text{initial}}$
198 ratios of 0.1294 to 0.1322. Such $^{187}\text{Os}/^{188}\text{Os}$ ratios range to more radiogenic values than estimates
199 of putative present-day primitive mantle (0.1296 ± 0.0008 , Meisel et al., 2001) but do not extend as
200 high as previous picrite data for the WG Vaigat formation (up to 0.1371, Schaefer et al., 2000) or
201 recent picrites from Iceland erupted within the last 1 Ma (up to 0.1378, Brandon et al., 2007).

202 Figure 2 here.

203 There is no co-variation of $^{187}\text{Os}/^{188}\text{Os}$ with Os concentration in either BI or WG picrites (Figure 3,
204 excluding CS-7, already discussed). Significant assimilation of crust or sub-continental lithospheric
205 mantle (SCLM) would likely result in samples from the same parental melt falling on mixing lines
206 towards either an Os-poor, ancient, extremely radiogenic crustal component or an Os-rich, ^{187}Os -
207 depleted SCLM; such trends are not observed. Equally, different parental melts would be variably
208 susceptible to contamination, according to their Os concentrations, and thus display a range of
209 isotope compositions. Previous WG data display increased $^{187}\text{Os}/^{188}\text{Os}$ in samples with <0.5 ng/g
210 Os (Schaefer et al., 2000), suggesting that Os-poor samples may be affected by crustal assimilation
211 and/or preferential sampling of radiogenic material during mantle melting; these samples have been
212 omitted from subsequent figures.

213 Figure 3 here.

214 **5. Discussion**

215 **5.1 Re-Os elemental behaviour**

216 Olivine accumulation in the NA picrites studied is indicated by sample MgO contents of up to 27.0
217 wt. %, compared to an estimated parental magma of 18-21 wt. % MgO (Pedersen, 1985; Larsen and
218 Pedersen, 2000; Herzberg and O'Hara, 2002). Osmium concentrations decrease with decreasing
219 MgO (Figure 1) and with Ni (not shown), reflecting the compatibility of Os within the olivine-rich
220 crystallising assemblage, which probably includes significant co-precipitated sulphide (as in global
221 MORB and OIB, e.g. Burton et al., 2002). Therefore, Os concentrations are likely controlled by
222 olivine accumulation and fractionation. On the basis of the Os content at MgO = 18 wt %, BI and
223 WG parental melts are estimated to contain ~ 1 and ~ 1.7 ng/g Os, respectively (Figure 1). As Os has

224 a high sulphide-silicate melt partition coefficient (at low pressures, e.g. ~10,000, Crocket et al.,
225 1997), such high parental melt Os concentrations probably require complete consumption of
226 sulphides in at least part of the melting column. The consumption of sulphide in a fertile upper
227 mantle source is thought to occur at melt fractions of >20-25%, based on the sulphide content of the
228 mantle and sulphur solubility in mafic melts (e.g. Mavrogenes and O'Neill, 1999; Lorand et al.,
229 2003), or at lower melt fractions for a previously depleted mantle source as proposed for the NA
230 picrites (e.g. Ellam and Stuart, 2004). These melt fractions are consistent with estimates based on
231 MgO content: ~20-28% for a fertile source or 10-11% for a depleted source (Herzberg and O'Hara,
232 2002). In addition to sulphide-silicate partitioning, physical entrainment of liquid sulphide within a
233 large degree silicate melt (Ballhaus et al., 2006) may, at least in part, account for the very high Os
234 concentrations of the NA picrite parental melts.

235 Rhenium concentrations in the picrites are lower than MORB, consistent with the moderate
236 incompatibility of Re during mantle melting and the higher melt fraction of picritic melts. Re/Yb
237 ratios are comparable to MORB (~0.00025), illustrating that Re maintains similar compatibility to
238 Yb at higher melt fractions than MORB. The preference of Re for olivine-poorer assemblages is
239 illustrated by increasing Re and Re/Os ratios with decreasing MgO content in almost all the picrite
240 units.

241 **5.2 Osmium-neodymium isotope systematics**

242 The majority of NA picrites analysed here have $^{143}\text{Nd}/^{144}\text{Nd}_{\text{initial}}$ of ~0.51307 (Graham et al., 1998;
243 Starkey et al., 2008, in press), consistent with a source dominated by a depleted mantle component,
244 as previously noted by Holm et al. (1993). Such Nd isotope compositions are indistinguishable
245 from the range of estimates for DMM corrected to 60 Ma (0.51304 - 0.51311, Salters and Stracke,
246 2004; Workman and Hart, 2005) and the proposed depleted end-member of the Iceland array (e.g.
247 Taylor et al., 1997). There is considerable $^{143}\text{Nd}/^{144}\text{Nd}$ variation in BI and Anaanaa (WG) picrites,

248 while $^{187}\text{Os}/^{188}\text{Os}$ is largely constant at around 0.127 (Figure 4). The $^{143}\text{Nd}/^{144}\text{Nd}$ range may be
249 partially due to crustal contamination (samples CS-7, 400444, Starkey et al., 2008, in press; and by
250 inference 408001.233) but still remains significant (0.512845 – 0.513072). In contrast, the younger
251 Ordlingassoq Member of the WG suite displays a negative co-variation of Os and Nd isotopes with
252 $^{143}\text{Nd}/^{144}\text{Nd}$ decreasing from 0.51308 to 0.51291 as $^{187}\text{Os}/^{188}\text{Os}$ increases from 0.1267 to 0.1322
253 (Figure 4). Literature data for the Naujánguit and Ordlingassoq Members (Schaefer et al., 2000),
254 possess similar systematics to the Ordlingassoq samples in this study, but display greater scatter,
255 probably due to careful screening during our sample selection to avoid potential crustal
256 contamination.

257 **5.2.1 Assessing the effects of post-melting crustal or lithospheric interaction**

258 Assessment of the potential effects of continental crust assimilation is of particular importance due
259 to the Proterozoic age of the crust through which the NA picrites were erupted. Careful screening
260 has removed samples which appear obviously contaminated by crust, but quantitative assessment of
261 the isotopic effects of minor contamination by continental crust is not a simple task due to its
262 marked heterogeneity, particularly in terms of Re-Os (e.g. Peucker-Ehrenbrink and Jahn, 2001).
263 The Os isotope composition of local crust has not been measured, and measurements, even if
264 numerous, are unlikely to provide a sufficiently well-constrained average due to the varied
265 basement geology. Baffin Island Proterozoic basement rocks also display a considerable range of
266 $^{143}\text{Nd}/^{144}\text{Nd}$ and Nd concentrations (Theriault et al., 2001), as do local Cretaceous West Greenland
267 sediments, derived from Proterozoic basement, which are the most likely contaminants (Goodrich
268 and Patchett, 1991, Larsen, unpubl.). Estimated Re and Os concentrations (Table 2) have been used
269 to calculate the $^{187}\text{Os}/^{188}\text{Os}$ composition of 2 Ga basement or basement-derived sediment, which has
270 then been combined with average measured Nd concentrations and isotope compositions (Table 2).

271 Mixing of average/best estimate 2 Ga basement or sedimentary cover with parental picritic melt
272 does not generate the uniform $^{187}\text{Os}/^{188}\text{Os}$ BI array, nor the negative co-variation of Nd and Os
273 isotopes observed in Ordlingassoq picrites. However, approximately 5% assimilation of two
274 different extreme crustal components may be able to account for both the BI and Ordlingassoq co-
275 variations (low Sm/Nd - low Re/Os and high Sm/Nd - high Re/Os crust, respectively, Figure 4), but
276 such very different and extreme contaminants are considered unlikely given the similar average
277 composition of the country rock in the two regions. Crust-melt mixing may also result in co-
278 variation of $^{187}\text{Os}/^{188}\text{Os}$ with Os concentration and this is not observed (Figure 3).

279 Combining Nd isotopes and Nb/Zr ratios provides a further line of evidence that crustal assimilation
280 is not a significant factor in controlling the isotope compositions of NA picrites (Starkey et al.,
281 2008, in press). The broad array of increasing Nb/Zr with decreasing $^{143}\text{Nd}/^{144}\text{Nd}$ cannot be
282 accounted for by assimilation of any low-Sm/Nd crustal material. Very small amounts of crustal
283 contamination can explain some of the spread in $^{143}\text{Nd}/^{144}\text{Nd}$, but Nd isotopes (and by inference Os
284 isotopes) predominantly reflect the mantle source.

285 Figure 4 here.

286 **5.2.2 Generation of the osmium and neodymium isotope variations in the mantle source**

287 The upper part of the Vaigat formation (WG) records increasing $^{187}\text{Os}/^{188}\text{Os}$ combined with
288 decreasing $^{143}\text{Nd}/^{144}\text{Nd}$. If this is unlikely to result from melt-crust interaction, such a shift in Os
289 and Nd isotope compositions may reflect an increased source input from an enriched component.
290 For instance, modelled mixing of DMM with 2 Ga recycled oceanic crust and associated sediment
291 can broadly produce the negative array in Os-Nd isotope space (Figure 4, e.g. ~5% recycled
292 component containing ~10% sediment). However, this model is non-unique and it is possible that
293 other enriched material such as metasomatised oceanic lithosphere (e.g. Niu and O'Hara, 2003)
294 could produce the negative array. Equally, mixtures of a hybrid putative primitive mantle –

295 recycled oceanic crust component with DMM can also explain the arrays of both the Ordlingassoq
296 and Iceland picrites, by varying the proportions of primitive mantle and recycled crust in the hybrid
297 component (Figure 4).

298 The variation of $^{143}\text{Nd}/^{144}\text{Nd}$ with no complementary change in $^{187}\text{Os}/^{188}\text{Os}$ seen in Baffin and
299 Anaanaa picrites is more difficult to explain because old recycled oceanic crust (plus sediment), and
300 old continental crust, are both likely to possess complementary high $^{187}\text{Os}/^{188}\text{Os}$ and low
301 $^{143}\text{Nd}/^{144}\text{Nd}$. Mixing of primitive mantle and DMM may be able to account for such an array
302 (Figure 4). Alternatively, such a signature may reflect a mantle source containing a minor
303 (sulphide-poor?) pyroxenite component that, due to its high Nd content and low Os content,
304 significantly affected the Nd isotope composition of the melt without noticeably affecting Os.
305 Regardless of the ultimate source of Nd isotope heterogeneity, the uniform $^{187}\text{Os}/^{188}\text{Os}$ of BI and
306 early WG picrites indicates that any enriched component has had little influence on Os isotope
307 compositions.

308 **5.3 Summarised evolution of the Iceland plume: Os, Nd and He evidence**

309 Volcanism associated with the onset of the proto-Iceland plume was derived from high degree
310 melting and was characterised by approximately chondritic Os isotope compositions, the highest
311 known $^3\text{He}/^4\text{He}$ ratios and variable, but fairly radiogenic $^{143}\text{Nd}/^{144}\text{Nd}$ ratios. Osmium isotope
312 compositions are consistent with a source more depleted than estimates of PUM (e.g. Meisel et al.,
313 2001), with no significant contribution from any enriched component including, based on current
314 models, the outer core (e.g. Walker et al., 1995; Brandon et al., 1998) or metasomatic sulphide
315 (Luguet et al., 2008b). Subsequent melts (Ordlingassoq Member), erupted within 1 Ma of the
316 earliest picrites, have elevated $^{187}\text{Os}/^{188}\text{Os}$ indicating a contribution from enriched material, possibly
317 old recycled oceanic crust plus sediment, which was not tapped in the first phase of plume melting,
318 but was soon brought into the zone of melting presumably by continued upwelling. Crustal and

319 lithospheric interactions appear to mask the source composition of 58 Ma East Greenland samples
320 (e.g. Peate et al., 2003), but $^3\text{He}/^4\text{He}$ up to 21 R_a has been measured (Marty et al., 1998).

321 Elevated $^{187}\text{Os}/^{188}\text{Os}$ ratios and low $^{143}\text{Nd}/^{144}\text{Nd}$ isotope data, relative to DMM, in recent Iceland
322 picrites (Brandon et al., 2007) can be explained by mixing of a similar recycled crustal component,
323 including ~5% sediment, with a DMM component (Figure 4). The absence of ^{186}Os enrichment in
324 these picrites, relative to DMM (Brandon et al., 2007), combined with the NA picrite Os data,
325 suggests no bulk core contribution to the plume over its history. High $^3\text{He}/^4\text{He}$ ratios persist in the
326 Iceland plume today (>30 R_a , Macpherson et al., 2005) and, intriguingly, $^3\text{He}/^4\text{He}$ increases with
327 $^{187}\text{Os}/^{188}\text{Os}$ in recent picrites (Brandon et al., 2007; Figure 6b), despite the proposed involvement of
328 recycled oceanic crust which would possess very low $^3\text{He}/^4\text{He}$ (~4, Brandon et al., 2007).

329 **5.4 The $^{187}\text{Os}/^{188}\text{Os}$ composition of shallow convecting mantle**

330 Trace element and Nd-Sr isotope evidence (Holm et al., 1993; Stuart et al., 2003; Ellam and Stuart,
331 2004; Kent et al., 2004) indicates that the early NA picrite source is typically depleted with respect
332 to putative primitive mantle (e.g. Zindler and Hart, 1986), and is indistinguishable from the MORB
333 source mantle (DMM, e.g. Salters and Stracke, 2004; Workman and Hart, 2005). The $^{187}\text{Os}/^{188}\text{Os}$
334 compositions of the earliest NA picrites (0.1267 to 0.1280) are consistent with a depleted mantle
335 source containing no significant contribution from recycled crust, pyroxenite, sediment, recycled
336 SCLM, metasomatised peridotite or outer core, nor any isolated ancient depleted domains.

337 Global ocean island basalts have variable reference TiO_2 concentrations (defined as the TiO_2
338 concentration on the olivine control line at the estimated parental MgO content). This has been
339 interpreted to reflect variable source contributions from enriched components, primarily recycled
340 oceanic crust (Prytulak and Elliott, 2007). The reference TiO_2 content for the early NA picrites is
341 $\leq 1\%$ (at ~18 wt. % MgO), lower than all OIB suites compiled by Prytulak and Elliott (2007), and
342 comparable to Iceland. By this measure the NA picrites define the least enriched end-member for

343 within plate magmas, i.e. their sources are dominated by peridotite, with minimal ‘enriched’
344 component. This conclusion is also supported by the low Ni/Mg ratios of Fo-rich picritic olivines
345 (0.74-0.94, Fo: 89-91, respectively; Larsen and Pedersen, 2000) which are comparable to MORB
346 and peridotite but lower than most within-plate magmas (Sobolev et al., 2007). Although Ni/Mg in
347 olivine may simply reflect the depth of melting, with which it appears positively correlated (Niu and
348 O'Hara, 2007), low Ni/Mg ratios combined with relatively deep melting definitely suggests an
349 insignificant pyroxenite source contribution.

350 Due to the large degree of melting during the generation of the NA picrites, their Os isotope
351 composition will closely reflect the composition of the bulk mantle source. This, coupled with the
352 chemical similarity to DMM and insignificance of enriched components, gives the potential for
353 providing an estimate of the bulk $^{187}\text{Os}/^{188}\text{Os}$ composition of the peridotitic convecting upper
354 mantle/DMM sampled by these magmas. The dominance of the DMM signature, in a proposed
355 plume-head, has probably arisen from extensive entrainment during the latter stages of plume
356 upwelling, and a disproportionate contribution due to melting in the shallower part of the melting
357 column. To facilitate comparison with other data such as those for MORB, initial $^{187}\text{Os}/^{188}\text{Os}$ for
358 picrites, platinum-group alloys and chromites have been recalculated to the present day by assuming
359 chondritic evolution of their sources since the time of mantle melting (Figure 5). Strictly speaking,
360 post-melting evolution of Os isotopes will be depressed relative to chondrite, due to Re depletion.
361 Thus, for a depleted NA picrite mantle source, with 0.12 ng/g Re (Sun et al., 2003), the present day
362 $^{187}\text{Os}/^{188}\text{Os}$ would be lower by 0.0002 than the values discussed below.

363 On the basis of the probability peak for the NA picrites, the $^{187}\text{Os}/^{188}\text{Os}$ composition of present day
364 convecting mantle underlying this region is estimated to be 0.1276 ± 0.0007 (2SD of data
365 contributing to peak, Figure 5). This value is indistinguishable from the least radiogenic recent
366 Iceland melts (<0.5 Ma, Skovgaard et al., 2001, Figure 3) and from the largest platinum-group alloy

367 peak (0.1276), derived mainly from Tibetan ophiolites (Pearson et al., 2007; Shi et al., 2007).
368 Phanerozoic ophiolite-derived chromites define a peak $^{187}\text{Os}/^{188}\text{Os}$ of 0.1283, while regression of
369 $^{187}\text{Os}/^{188}\text{Os}$ versus time gives a lower intercept of 0.1281 (Walker et al., 2002b). Subduction-related
370 enrichment of Re (see Becker, 2000; Dale et al., 2007) or radiogenic Os (e.g. Brandon et al., 1996)
371 has the potential to elevate this value, although this must also be considered for the ophiolite-
372 derived platinum-group alloys. The $^{187}\text{Os}/^{188}\text{Os}$ estimate defined by NA picrites and platinum-
373 group alloys is intermediate between averages for carbonaceous, enstatite and ordinary chondrites
374 (0.1262, 0.1281, 0.1283, respectively, Walker et al., 2002a). It is, however, significantly lower than
375 the proposed $^{187}\text{Os}/^{188}\text{Os}$ of 0.1296 ± 0.0008 for putative PUM, based on co-variation of Al_2O_3 and
376 $^{187}\text{Os}/^{188}\text{Os}$ in mantle xenoliths (Meisel et al., 2001). This difference is presumably due to the effect
377 of time-integrated mantle Re depletion through the generation of continental crust and/or generation
378 and isolation of subducted oceanic crust, although the potential effects of coupled metasomatic
379 increases in Al_2O_3 (e.g. Pearson et al., 2003) and $^{187}\text{Os}/^{188}\text{Os}$ (e.g. Alard et al., 2005) may also need
380 to be considered. The similarity between the modal NA picrite Os isotope composition and other
381 estimates of convecting mantle indicate that a $^{187}\text{Os}/^{188}\text{Os}$ value somewhere between 0.1274 and
382 0.1281 might be an appropriate estimate for ambient shallow convecting mantle.

383 Figure 5 here.

384 The least radiogenic MORB ($^{187}\text{Os}/^{188}\text{Os}$ of 0.1261-0.1272) are isotopically similar to the NA
385 picrite $^{187}\text{Os}/^{188}\text{Os}$ peak of 0.1276, and therefore support this proposal. Most MORB are
386 significantly more radiogenic with $^{187}\text{Os}/^{188}\text{Os}$ ratios up to 0.148 (Gannoun et al., 2007). This
387 probably reflects preferential sampling of enriched components and/or ^{187}Os -rich metasomatic
388 sulphides within the DMM, by MORB melts of smaller degree than the NA picrites (e.g. Alard et
389 al., 2005; Escrig et al., 2005). If such enriched components are present in the initial NA picrite

390 source (as suggested by the Nd isotope data), their Os isotope signature is greatly diluted compared
391 to the contribution from depleted peridotite.

392 **5.5 Implications for high $^3\text{He}/^4\text{He}$ in the mantle**

393 Based on the possibility of greater compatibility of He than U and Th during mantle melting
394 (Graham et al., 1990; Parman et al., 2005; Heber et al., 2007), it has been proposed that ancient melt
395 depletion will lead to the retention of high $^3\text{He}/^4\text{He}$ in the residue, through reduced ingrowth of ^4He
396 (Class and Goldstein, 2005; Parman et al., 2005). The timing of this depletion event, for $^3\text{He}/^4\text{He}$ as
397 high as $50 R_a$, has been variously estimated at 3.7 and 3.1 Ga (Parman, 2007; Porcelli and Elliott,
398 2008). Preservation of high $^3\text{He}/^4\text{He}$ through depletion probably requires a large degree of melting
399 (Parman et al., 2005; Porcelli and Elliott, 2008) and this would likely result in near complete Re
400 depletion. Depletion of Re during such mantle melting will lead, over time, to $^{187}\text{Os}/^{188}\text{Os}$ ratios
401 which deviate well below the chondrite evolution curve. Thus, in contrast to the broadly chondritic
402 $^{187}\text{Os}/^{188}\text{Os}$ of the NA picrites, a source entirely depleted in Re at 3.7 or 3.1 Ga (T_{RD}), and
403 subsequently isolated, would have $^{187}\text{Os}/^{188}\text{Os}$ of ~ 0.102 or ~ 0.107 , respectively. Even partial Re
404 depletion of the source at these ages would reduce $^{187}\text{Os}/^{188}\text{Os}$ evolution to between 0.113 and
405 0.115 (if Re was reduced to 0.12 ng/g, equal to an estimate of the DMM (Sun et al., 2003), Figure
406 6). The lowest initial $^{187}\text{Os}/^{188}\text{Os}$ for the NA picrites corresponds to a T_{RD} of only ~ 0.4 Ga, and
407 therefore Os isotopes are not consistent with ancient depletion as a mechanism for the preservation
408 of the highest known mantle $^3\text{He}/^4\text{He}$ ratios. Equally, mixing of high $^3\text{He}/^4\text{He}$ depleted mantle and
409 DMM entrained in the plume, cannot explain the range of $^3\text{He}/^4\text{He}$ at a near constant $^{187}\text{Os}/^{188}\text{Os}$ as
410 the former is unlikely to have a sufficiently high He content (Figure 6). Alternative models, such as
411 a sub-continental lithospheric mantle source for the high $^3\text{He}/^4\text{He}$ are also not supported by the Os
412 isotope data, because they too demand significantly sub-chondritic $^{187}\text{Os}/^{188}\text{Os}$ (see Larsen et al.,
413 2003 for WG lithosphere). Furthermore, high $^3\text{He}/^4\text{He}$ has not been found in sub-continental mantle
414 xenoliths or melts (Dunai and Baur, 1995; Day et al., 2005). For the NA picrites considered here,

415 only subsequent addition of radiogenic Os, without He, could reconcile the Os data with an ancient
416 depleted source for the high $^3\text{He}/^4\text{He}$. Such a specific flux seems unlikely as fluid-mobile or
417 incompatible elements, including both U and Th, and probably He, would also presumably be
418 involved.

419 Figure 6 here.

420 Table 2 here.

421 The core has been proposed as a possible source of He enriched in ^3He (e.g. Macpherson et al.,
422 1998; Porcelli and Halliday, 2001). The proposed partitioning behaviour of Re and Os between the
423 inner and outer core has led to the hypothesis that the outer core possesses supra-chondritic Re/Os
424 ratios (Walker et al., 1995). Based on this model, the approximately chondritic $^{187}\text{Os}/^{188}\text{Os}$ of high
425 $^3\text{He}/^4\text{He}$ NA picrites precludes a bulk contribution from core material, as much less than 1% Fe-rich
426 core input would impart a radiogenic signature due to its much greater Os concentration. However,
427 decoupled transfer of He and Os across the core-mantle boundary, for instance by diffusion, could
428 produce high $^3\text{He}/^4\text{He}$ without correspondingly high $^{187}\text{Os}/^{188}\text{Os}$.

429 In an attempt to account for the Os-He isotope data, mixing calculations for various possible mantle
430 components have been performed (Figure 6). However, constraints on He abundances are poor and
431 can be varied in order to better fit the data. We find such flexibility unsatisfactory in that it leads to
432 non-uniquely constrained models, thus we have cautious conclusions from our modelling.

433 Furthermore, such modelling implicitly assumes that source contributions of He and Os are
434 coupled, while the parameters are not sufficiently constrained to allow assessment of this
435 assumption.

436 Mixing between DMM and a subsidiary primitive mantle component (up to 25% in this model) can
437 broadly explain the Os-He array for the picrites with constant, approximately chondritic $^{187}\text{Os}/^{188}\text{Os}$
438 (Figure 6). A primitive high $^3\text{He}/^4\text{He}$ source of >50 with sufficient He, would permit a small
439 contribution derived from 2 Ga recycled oceanic crust, while retaining $^3\text{He}/^4\text{He}$ of >45 as observed
440 in some WG Ordingassoq picrites (also proposed for Iceland, Brandon et al., 2007). However, the
441 difference in He concentration between a proposed primitive mantle-recycled oceanic crust end-
442 member and DMM gives rise to convex-up mixing curves which means that Ordingassoq samples
443 require unique proportions of primitive mantle, recycled oceanic crust and DMM, rather than
444 variable contributions along a single mixing line. Convex-up mixing lines are also problematic for
445 the quasi-linear Icelandic array, although use of a higher He concentration for the DMM than that
446 used by Brandon et al. (2007) (Table 2), generates mixing lines that more closely approach linearity
447 (Figure 6). Mixing of DMM, PM and recycled oceanic crust plus sediment can also broadly explain
448 the NA and Iceland picrite Os-Nd variations (Figure 4), but such mixing requires somewhat
449 different component proportions in Os-He and Os-Nd isotope space and does not easily account for
450 each individual sample.

451 It has been proposed that a high $^3\text{He}/^4\text{He}$ component could be widespread in the upper mantle
452 (Meibom et al., 2003), and such a component with MORB-like $^{187}\text{Os}/^{188}\text{Os}$ of ~ 0.1276 cannot be
453 ruled out on the basis of these data, as long as it contains sufficient He to retain high $^3\text{He}/^4\text{He}$
454 despite mixing of a minor recycled oceanic crust component. However, while the mechanisms for
455 such a scenario are not well understood, it seems unlikely that this material would only be sampled
456 during episodes of large degree melting of hot mantle (as opposed to MORB melting) and even if
457 so, that it would not also impart an ancient depleted Os isotope signature, complementary to the
458 unradiogenic high $^3\text{He}/^4\text{He}$ signature.

459 Given that high $^3\text{He}/^4\text{He}$ ratios (>45) in NA picrites are not restricted to samples with a specific Os
460 isotope signature and mixing models do not satisfactorily explain isotope co-variations in detail, it
461 seems most likely that Os and He are decoupled (and Nd-He, Starkey et al., 2008, in press).
462 Diffusion or mixing of high $^3\text{He}/^4\text{He}$ from a He-rich primordial reservoir could impart the necessary
463 He signature without significantly changing the previously established Os and Nd isotope
464 heterogeneity. Constraining the ultimate source of this high $^3\text{He}/^4\text{He}$ component is difficult, but as
465 it was tapped most efficiently during melting of a plume-head and persists in Icelandic volcanism
466 today, it seems most plausible that it diffused across, or was entrained at, a deep boundary layer.

467 **6. Concluding remarks**

468 Osmium concentrations in NA picrites are high for mantle melts (1-1.7 ng/g parental Os content)
469 and suggest complete consumption of sulphide in at least part of the source due to a large degree of
470 melting. This is consistent with previous evaluations of the degree of melting based on MgO-rich
471 olivines: 10-11% for depleted mantle (Herzberg and O'Hara, 2002). Initial Os isotope compositions
472 in the earliest picrite melts from West Greenland (early Vaigat formation) and Baffin Island are
473 uniform and broadly chondritic (probability peak of $^{187}\text{Os}/^{188}\text{Os} = 0.1272$). In terms of Os isotope
474 mass balance, this initial volcanism cannot contain any significant contribution from the outer core
475 or from old recycled crustal material, as both would impart a radiogenic $^{187}\text{Os}/^{188}\text{Os}$ signature. In
476 addition, the minimal presence of enriched pyroxenitic components in the source of NA picrites is
477 suggested by various parameters such as Ni content of olivine and bulk-rock TiO_2 content. The
478 absence of enriched components, coupled with a large degree of melting and Nd isotope
479 compositions which are indistinguishable from DMM, means that the average $^{187}\text{Os}/^{188}\text{Os}$ may
480 reflect the bulk $^{187}\text{Os}/^{188}\text{Os}$ of convecting mantle. This value, when corrected to the present day, is
481 similar to the least radiogenic MORB (e.g. Gannoun et al., 2007) and the most common $^{187}\text{Os}/^{188}\text{Os}$
482 ratios found in platinum-group alloys from Tibetan ophiolites (Pearson et al., 2007; Shi et al.,

483 2007). Subsequent melts sampled from the upper Vaigat formation, erupted within 1 Ma of the
484 earliest melts (Storey et al., 1998), possess supra-chondritic initial $^{187}\text{Os}/^{188}\text{Os}$ ratios of up to
485 0.1321. Such ratios, also seen in recent Iceland plume melts (Brandon et al., 2007), can be
486 accounted for (though not uniquely) by a greater contribution from recycled oceanic crust.

487 Models seeking to explain high mantle $^3\text{He}/^4\text{He}$ ratios by ancient depletion (Class and Goldstein,
488 2005; Parman, 2007) are not supported by the uniform and largely chondritic $^{187}\text{Os}/^{188}\text{Os}$ ratios of
489 NA picrites. Ancient melting and isolation would lead to significantly sub-chondritic $^{187}\text{Os}/^{188}\text{Os}$ in
490 the NA picrite source, which possesses the highest known mantle-derived $^3\text{He}/^4\text{He}$ ratios (up to 50
491 R_a , Stuart et al., 2003). Outer core material would nominally impart radiogenic Os to the plume,
492 and so core material is also not supported as a source of high $^3\text{He}/^4\text{He}$, unless the mechanism of He
493 transfer to the plume (diffusion?) is decoupled from Os. Therefore, three possible explanations for
494 the high $^3\text{He}/^4\text{He}$ signature are: (i) it is present in a typical upper mantle source, entrained in the
495 plume-head, but is only tapped during episodes of high-degree melting of hot mantle; (ii) it is
496 derived from a primitive mantle component which has been mixed with recycled oceanic crust and
497 DMM in order to broadly explain the Os, He and Nd isotope variations or, (iii) He is largely
498 decoupled from Os and Nd and is dominated by addition of a He-rich, high $^3\text{He}/^4\text{He}$ component,
499 probably primordial in nature, without complementary addition of other elements. The difficulties
500 presented above for (i) and (ii) and the fact that high $^3\text{He}/^4\text{He}$ is not restricted to a source with a
501 particular Os (or Nd) isotope composition make the latter our favoured model.

502 **Acknowledgements**

503 C. Dale thanks the Natural Environment Research Council (NERC) for supporting this work as part
504 of standard grant, NE/C51902x/1. We are grateful to Sarah Woodland for some Os isotope
505 analyses and to Chris Ottley for assistance with Re measurements. The first collection of Baffin
506 Island samples was partly funded by The Sheila Hall Trust (now Laidlaw-Hall Trust); Don Francis

507 organised the second collection. We thank two anonymous reviewers and R. Carlson for their
508 thorough reviews which have improved the manuscript significantly.

509 main text: 6380

510

511

512 **References**

- 513 Alard, O., Luguet, A., Pearson, N.J., Griffin, W.L., Lorand, J.P., Gannoun, A., Burton, K.W. and
514 O'Reilly, S.Y., 2005. In situ Os isotopes in abyssal peridotites bridge the isotopic gap
515 between MORBs and their source mantle. *Nature*, 436(7053): 1005-1008.
- 516 Ballhaus, C., Bockrath, C., Wohlgemuth-Ueberwasser, C., Laurenz, V. and Berndt, J., 2006.
517 Fractionation of the noble metals by physical processes. *Contributions to Mineralogy and*
518 *Petrology*, 152(6): 667-684.
- 519 Becker, H., 2000. Re-Os fractionation in eclogites and blueschists and the implications for recycling
520 of oceanic crust into the mantle. *Earth and Planetary Science Letters*, 177(3-4): 287-300.
- 521 Becker, H., Horan, M.F., Walker, R.J., Gao, S., Lorand, J.P. and Rudnick, R.L., 2006. Highly
522 siderophile element composition of the Earth's primitive upper mantle: Constraints from
523 new data on peridotite massifs and xenoliths. *Geochimica Et Cosmochimica Acta*, 70(17):
524 4528-4550.
- 525 Bennett, V.C., Esat, T.M. and Norman, M.D., 1996. Two mantle-plume components in Hawaiian
526 picrites inferred from correlated Os-Pb isotopes. *Nature*, 381(6579): 221-224.
- 527 Brandon, A.D., Creaser, R.A., Shirey, S.B. and Carlson, R.W., 1996. Osmium recycling in
528 subduction zones. *Science*, 272(5263): 861-864.
- 529 Brandon, A.D., Walker, R.J., Morgan, J.W., Norman, M.D. and Prichard, H.M., 1998. Coupled
530 ^{186}Os and ^{187}Os evidence for core-mantle interaction. *Science*, 280(5369): 1570-1573.
- 531 Brandon, A.D., Snow, J.E., Walker, R.J., Morgan, J.W. and Mock, T.D., 2000. ^{190}Pt - ^{186}Os and
532 ^{187}Re - ^{187}Os systematics of abyssal peridotites. *Earth and Planetary Science Letters*, 177(3-
533 4): 319-335.
- 534 Brandon, A.D., Graham, D.W., Waight, T. and Gautason, B., 2007. ^{186}Os and ^{187}Os enrichments
535 and high- $^3\text{He}/^4\text{He}$ sources in the Earth's mantle: Evidence from Icelandic picrites.
536 *Geochimica et Cosmochimica Acta*, 71(18): 4570-4591.
- 537 Burton, K.W., Gannoun, A., Birck, J.-L., Allegre, C.J., Schiano, P., Clocchiatti, R. and Alard, O.,
538 2002. The compatibility of rhenium and osmium in natural olivine and their behaviour
539 during mantle melting and basalt genesis. *Earth and Planetary Science Letters*, 198(1-2): 63-
540 76.
- 541 Class, C. and Goldstein, S.L., 2005. Evolution of helium isotopes in the Earth's mantle. *Nature*,
542 436(7054): 1107-1112.
- 543 Cohen, A.S. and Waters, F.G., 1996. Separation of osmium from geological materials by solvent
544 extraction for analysis by thermal ionisation mass spectrometry. *Analytica Chimica Acta*,
545 332(2-3): 269-275.

- 546 Crocket, J.H., Fleet, M.E. and Stone, W.E., 1997. Implications of composition for experimental
547 partitioning of platinum-group elements and gold between sulfide liquid and basalt melt:
548 The significance of nickel content. *Geochimica Et Cosmochimica Acta*, 61(19): 4139-4149.
- 549 Dale, C.W., Gannoun, A., Burton, K.W., Argles, T.W. and Parkinson, I.J., 2007. Rhenium–osmium
550 isotope and elemental behaviour during subduction of oceanic crust and the implications for
551 mantle recycling. *Earth and Planetary Science Letters*, 253: 211-225.
- 552 Dale, C.W., Luguet, A., Macpherson, C.G., Pearson, D.G. and Hickey-Vargas, R., 2008. Extreme
553 platinum-group element fractionation and variable Os isotope compositions in Philippine
554 Sea Plate basalts: Tracing mantle source heterogeneity. *Chemical Geology*, 248(3-4): 213-
555 238.
- 556 Dale, C.W., Burton, K.W., Pearson, D.G., Gannoun, A., Alard, O., Argles, T.W. and Parkinson, I.J.,
557 2008, in press. Highly siderophile element behaviour accompanying subduction of oceanic
558 crust: whole rock and mineral-scale insights from a high-pressure terrain. *Geochimica et*
559 *Cosmochimica Acta*.
- 560 Day, J.M.D., Hilton, D.R., Pearson, D.G., Macpherson, C.G., Kjarsgaard, B.A. and Janney, P.E.,
561 2005. Absence of a high time-integrated He-3/(U+Th) source in the mantle beneath
562 continents. *Geology*, 33(9): 733-736.
- 563 Dunai, T.J. and Baur, H., 1995. Helium, neon, and argon systematics of the European sub-
564 continental mantle - Implications for its geochemical evolution. *Geochimica et*
565 *Cosmochimica Acta*, 59(13): 2767-2783.
- 566 Ellam, R.M. and Stuart, F.M., 2004. Coherent He-Nd-Sr isotope trends in high He-3/He-4 basalts:
567 implications for a common reservoir, mantle heterogeneity and convection. *Earth and*
568 *Planetary Science Letters*, 228(3-4): 511-523.
- 569 Escrig, S., Schiano, P., Schilling, J.G. and Allegre, C., 2005. Rhenium-osmium isotope systematics
570 in MORB from the Southern Mid-Atlantic Ridge (40 degrees-50 degrees S). *Earth and*
571 *Planetary Science Letters*, 235(3-4): 528-548.
- 572 Francis, D., 1985. The Baffin-Bay Lavas and the Value of Picrites as Analogs of Primary Magmas.
573 *Contributions to Mineralogy and Petrology*, 89(2-3): 144-154.
- 574 Gannoun, A., Burton, K.W., Parkinson, I.J., Alard, O., Schiano, P. and Thomas, L.E., 2007. The
575 scale and origin of the osmium isotope variations in mid-ocean ridge basalts. *Earth and*
576 *Planetary Science Letters*, 259(3-4): 541-556.
- 577 Gill, R.C.O., Pedersen, A.K. and Larsen, J.G., 1992. Tertiary picrites in West Greenland: melting at
578 the periphery of a plume? In: B.C. Storey, T. Alabaster and R.J. Pankhurst (Editors),
579 *Magmatism and the causes of continental break-up*. Geol. Soc. London, Spec. Publ.

- 580 Goodrich, C.A. and Patchett, P.J., 1991. Nd and Sr isotope chemistry of metallic iron-bearing,
581 sediment-contaminated Tertiary volcanics from Disko Island, Greenland *Lithos*, 27(1): 13-
582 27.
- 583 Graham, D., Lupton, J., Albarede, F. and Condomines, M., 1990. Extreme Temporal Homogeneity
584 of Helium-Isotopes at Piton-De-La-Fournaise, Reunion Island. *Nature*, 347(6293): 545-548.
- 585 Graham, D.W., Larsen, L.M., Hanan, B.B., Storey, M., Pedersen, A.K. and Lupton, J.E., 1998.
586 Helium isotope composition of the early Iceland mantle plume inferred from the tertiary
587 picrites of West Greenland. *Earth and Planetary Science Letters*, 160(3-4): 241-255.
- 588 Graham, D.W., 2003. Noble Gas Isotope Geochemistry of Mid-Ocean Ridge and Ocean Island
589 Basalts: Characterization of Mantle Source Reservoirs. In: D. P. Porcelli, C.J. Ballentine and
590 R. Wieler (Editors), *Noble Gases. Reviews in Mineralogy and Geochemistry*, 47.
- 591 Harvey, J., Gannoun, A., Burton, K.W., Rogers, N.W., Alard, O. and Parkinson, I.J., 2006. Ancient
592 melt extraction from the oceanic upper mantle revealed by Re-Os isotopes in abyssal
593 peridotites from the Mid-Atlantic ridge. *Earth and Planetary Science Letters*, 244(3-4): 606-
594 621.
- 595 Hauri, E.H. and Hart, S.R., 1993. Re-Os Isotope Systematics of HIMU and EM-II Oceanic Island
596 Basalts from the South-Pacific Ocean. *Earth and Planetary Science Letters*, 114(2-3): 353-
597 371.
- 598 Hauri, E.H., Lassiter, J.C. and DePaolo, D.J., 1996. Osmium isotope systematics of drilled lavas
599 from Mauna Loa, Hawaii. *Journal of Geophysical Research-Solid Earth*, 101(B5): 11793-
600 11806.
- 601 Heber, V.S., Brooker, R.A., Kelley, S.P. and Wood, B.J., 2007. Crystal-melt partitioning of noble
602 gases (helium, neon, argon, krypton, and xenon) for olivine and clinopyroxene. *Geochimica
603 Et Cosmochimica Acta*, 71(4): 1041-1061.
- 604 Herzberg, C. and O'Hara, M.J., 2002. Plume-associated ultramafic magmas of phanerozoic age.
605 *Journal of Petrology*, 43(10): 1857-1883.
- 606 Holm, P.M., Gill, R.C.O., Pedersen, A.K., Larsen, J.G., Hald, N., Nielsen, T.F.D. and Thirlwall,
607 M.F., 1993. The Tertiary Picrites of West Greenland - Contributions from Icelandic and
608 Other Sources. *Earth and Planetary Science Letters*, 115(1-4): 227-244.
- 609 Kent, A.J.R., Stolper, E.M., Francis, D., Woodhead, J., Frei, R. and Eiler, J., 2004. Mantle
610 heterogeneity during the formation of the North Atlantic Igneous Province: Constraints from
611 trace element and Sr-Nd-Os-O isotope systematics of Baffin Island picrites. *Geochemistry
612 Geophysics Geosystems*, 5.
- 613 Kurz, M.D., Jenkins, W.J. and Hart, S.R., 1982. Helium Isotopic Systematics of Oceanic Islands
614 and Mantle Heterogeneity. *Nature*, 297(5861): 43-47.

- 615 Larsen, L.M. and Pedersen, A.K., 2000. Processes in high-mg, high-T magmas: Evidence from
616 olivine, chromite and glass in palaeogene picrites from West Greenland. *Journal of*
617 *Petrology*, 41(7): 1071-1098.
- 618 Larsen, L.M., Pedersen, A.K., Sundvoll, B. and Frei, R., 2003. Alkali picrites formed by melting of
619 old metasomatized lithospheric mantle: Manitdlat member, Vaigat Formation, Palaeocene of
620 West Greenland. *Journal of Petrology*, 44(1): 3-38.
- 621 Lorand, J.P., Alard, O., Luguet, A. and Keays, R.R., 2003. Sulfur and selenium systematics of the
622 subcontinental lithospheric mantle: Inferences from the Massif Central xenolith suite
623 (France). *Geochimica Et Cosmochimica Acta*, 67(21): 4137-4151.
- 624 Luguet, A., Nowell, G.M. and Pearson, D.G., 2008a. $^{184}\text{Os}/^{188}\text{Os}$ and $^{186}\text{Os}/^{188}\text{Os}$ measurements by
625 Negative Thermal Ionisation Mass Spectrometry (N-TIMS): Effects of interfering element
626 and mass fractionation corrections on data accuracy and precision. *Chemical Geology*,
627 248(3-4): 342-362.
- 628 Luguet, A., Pearson, D.G., Nowell, G.M., Dreher, S.T., Coggon, J.A., Spetsius, Z.V. and Parman,
629 S.W., 2008b. Enriched Pt-Re-Os isotope systematics in plume lavas explained by
630 metasomatic sulfides. *Science*, 319(5862): 453-456.
- 631 Macpherson, C.G., Hilton, D.R., Sinton, J.M., Poreda, R.J. and Craig, H., 1998. High $^3\text{He}/^4\text{He}$ ratios
632 in the Manus backarc basin: Implications for mantle mixing and the origin of plumes in the
633 western Pacific Ocean. *Geology*, 26(11): 1007-1010.
- 634 Macpherson, C.G., Hilton, D.R., Day, J.M.D., Lowry, D. and Gronvold, K., 2005. High- $^3\text{He}/^4\text{He}$,
635 depleted mantle and low- $\delta\text{O}-18$, recycled oceanic lithosphere in the source of central
636 Iceland magmatism. *Earth and Planetary Science Letters*, 233(3-4): 411-427.
- 637 Marcantonio, F., Zindler, A., Elliott, T. and Staudigel, H., 1995. Os Isotope Systematics of La
638 Palma, Canary-Islands - Evidence for Recycled Crust in the Mantle Source of HIMU Ocean
639 Islands. *Earth and Planetary Science Letters*, 133(3-4): 397-410.
- 640 Martin, C.E., 1991. Osmium Isotopic Characteristics of Mantle-Derived Rocks. *Geochimica et*
641 *Cosmochimica Acta*, 55(5): 1421-1434.
- 642 Martin, C.E., Carlson, R.W., Shirey, S.B., Frey, F.A. and Chen, C.Y., 1994. Os-Isotopic Variation
643 in Basalts from Haleakala Volcano, Maui, Hawaii - a Record of Magmatic Processes in
644 Oceanic Mantle and Crust. *Earth and Planetary Science Letters*, 128(3-4): 287-301.
- 645 Marty, B., Upton, B.G.J. and Ellam, R.M., 1998. Helium isotopes in early tertiary basalts, northeast
646 Greenland: Evidence for 58Ma plume activity in the north Atlantic Iceland volcanic
647 province. *Geology*, 26(5): 407-410.
- 648 Mavrogenes, J.A. and O'Neill, H.S.C., 1999. The relative effects of pressure, temperature and
649 oxygen fugacity on the solubility of sulfide in mafic magmas. *Geochimica Et Cosmochimica*
650 *Acta*, 63(7-8): 1173-1180.

- 651 Meibom, A., Sleep, N.H., Chamberlain, C.P., Coleman, R.G., Frei, R., Hren, M.T. and Wooden,
652 J.L., 2002. Re-Os isotopic evidence for long-lived heterogeneity and equilibration processes
653 in the Earth's upper mantle. *Nature*, 419(6908): 705-708.
- 654 Meibom, A., Anderson, D.L., Sleep, N.H., Frei, R., Chamberlain, C.P., Hren, M.T. and Wooden,
655 J.L., 2003. Are high $^3\text{He}/^4\text{He}$ ratios in oceanic basalts an indicator of deep-mantle plume
656 components? *Earth and Planetary Science Letters*, 208(3-4): 197-204.
- 657 Meisel, T., Walker, R.J., Irving, A.J. and Lorand, J.P., 2001. Osmium isotopic compositions of
658 mantle xenoliths: A global perspective. *Geochimica Et Cosmochimica Acta*, 65(8): 1311-
659 1323.
- 660 Moreira, M., Breddam, K., Curtice, J. and Kurz, M.D., 2001. Solar neon in the Icelandic mantle:
661 new evidence for an undegassed lower mantle. *Earth and Planetary Science Letters*, 185(1-
662 2): 15-23.
- 663 Morgan, J.W., Walker, R.J., Brandon, A.D. and Horan, M.F., 2001. Siderophile elements in Earth's
664 upper mantle and lunar breccias: Data synthesis suggests manifestations of the same late
665 influx. *Meteoritics & Planetary Science*, 36(9): 1257-1275.
- 666 Niu, Y.L. and O'Hara, M.J., 2003. Origin of ocean island basalts: A new perspective from
667 petrology, geochemistry, and mineral physics considerations. *Journal of Geophysical
668 Research-Solid Earth*, 108(B4).
- 669 Niu, Y.L. and O'Hara, M.J., 2007. Varying Ni in OIB olivines - Product of process not source.
670 *Geochimica et Cosmochimica Acta*, 71(15): A721.
- 671 Parman, S.W., Kurz, M.D., Hart, S.R. and Grove, T.L., 2005. Helium solubility in olivine and
672 implications for high $\text{He-3}/\text{He-4}$ in ocean island basalts. *Nature*, 437(7062): 1140-1143.
- 673 Parman, S.W., 2007. Helium isotopic evidence for episodic mantle melting and crustal growth.
674 *Nature*, 446(7138): 900-903.
- 675 Pearson, D.G. and Woodland, S.J., 2000. Solvent extraction/anion exchange separation and
676 determination of PGEs (Os, Ir, Pt, Pd, Ru) and Re-Os isotopes in geological samples by
677 isotope dilution ICP-MS. *Chemical Geology*, 165(1-2): 87-107.
- 678 Pearson, D.G., Canil, D. and Shirey, S.B., 2003. Mantle samples included in volcanic rocks:
679 xenoliths and diamonds. In: R.W. Carlson, H.D. Holland and K.K. Turekian (Editors), *The
680 Mantle and Core, Treatise on Geochemistry*. Elsevier, Amsterdam pp. 171–275.
- 681 Pearson, D.G., Parman, S.W. and Nowell, G.M., 2007. A link between large mantle melting events
682 and continent growth seen in osmium isotopes. *Nature*, 449(7159): 202-205.
- 683 Peate, D.W., Baker, J.A., Blichert-Toft, J. et al., 2003. The Prinsen af Wales Bjerge formation
684 lavas, East Greenland: The transition from tholeiitic to alkalic magmatism during
685 Palaeogene continental break-up. *Journal of Petrology*, 44(2): 279-304.

- 686 Pedersen, A.K., 1985. Reaction between picrite magma and continental crust: early Tertiary silicic
687 basalts and magnesian andesites from Disko, West Greenland. *Bulletin Grønlands*
688 *Geologiske Undersøgelse*, 152: 126 pp.
- 689 Pedersen, A.K., Larsen, L.M., Riisager, P. and Dueholm, K.S., 2002. Rates of volcanic deposition,
690 facies changes and movements in a dynamic basin: the Nuussuaq Basin, West Greenland,
691 around the C27n-C26r transition. . In: D.W. Jolley and B.R. Bell (Editors), *The North*
692 *Atlantic Igneous Province: stratigraphy, tectonics, volcanic and magmatic processes.*
693 *Geological Society, London*, 197, pp. 157-181.
- 694 Peucker-Ehrenbrink, B. and Jahn, B.M., 2001. Rhenium-osmium isotope systematics and platinum
695 group element concentrations: Loess and the upper continental crust. *Geochemistry*
696 *Geophysics Geosystems*, 2: art. no.-2001GC000172.
- 697 Porcelli, D. and Halliday, A.N., 2001. The core as a possible source of mantle helium. *Earth and*
698 *Planetary Science Letters*, 192(1): 45-56.
- 699 Porcelli, D., Ballentine, C.J. and Wieler, R., 2002. An overview of noble gas - *Geochemistry and*
700 *cosmochemistry. Noble Gases in Geochemistry and Cosmochemistry*, 47: 1-19.
- 701 Porcelli, D. and Elliott, T., 2008. The evolution of He Isotopes in the convecting mantle and the
702 preservation of high He-3/He-4 ratios. *Earth and Planetary Science Letters*, 269(1-2): 175-
703 185.
- 704 Prytulak, J. and Elliott, T., 2007. TiO₂ enrichment in ocean island basalts. *Earth and Planetary*
705 *Science Letters*, 263(3-4): 388-403.
- 706 Reisberg, L., Zindler, A., Marcantonio, F., White, W., Wyman, D. and Weaver, B., 1993. Os
707 Isotope Systematics in Ocean Island Basalts. *Earth and Planetary Science Letters*, 120(3-4):
708 149-167.
- 709 Roy-Barman, M. and Allegre, C.J., 1994. ¹⁸⁷Os-¹⁸⁶Os Ratios of Midocean Ridge Basalts and
710 Abyssal Peridotites. *Geochimica et Cosmochimica Acta*, 58(22): 5043-5054.
- 711 Salters, V.J.M. and Stracke, A., 2004. Composition of the depleted mantle. *Geochemistry*
712 *Geophysics Geosystems*, 5: art. no.-Q05004.
- 713 Saunders, A.D., Fitton, J.G., Kerr, A.C., Norry, M.J. and Kent, R.W., 1997. The North Atlantic
714 Igneous Province. In: J.J. Mahoney and M.F. Coffin (Editors), *Large Igneous Provinces.*
715 *Geophysical monograph. Vol. 100*, pp. 45-94.
- 716 Schaefer, B.F., Parkinson, I.J. and Hawkesworth, C.J., 2000. Deep mantle plume osmium isotope
717 signature from West Greenland Tertiary picrites. *Earth and Planetary Science Letters*,
718 175(1-2): 105-118.
- 719 Shi, R.D., Alard, O., Zhi, X.C., O'Reilly, S.Y., Pearson, N.J., Griffin, W.L., Zhang, M. and Chen,
720 X.M., 2007. Multiple events in the Neo-Tethyan oceanic upper mantle: Evidence from Ru-

- 721 Os-Ir alloys in the Luobusa and Dongqiao ophiolitic podiform chromitites, Tibet. *Earth and*
722 *Planetary Science Letters*, 261(1-2): 33-48.
- 723 Shirey, S.B. and Walker, R.J., 1998. The Re-Os isotope system in cosmochemistry and high-
724 temperature geochemistry. *Annual Review of Earth and Planetary Sciences*, 26: 423-500.
- 725 Skovgaard, A.C., Storey, M., Baker, J., Blusztajn, J. and Hart, S.R., 2001. Osmium-oxygen isotopic
726 evidence for a recycled and strongly depleted component in the Iceland mantle plume. *Earth*
727 *and Planetary Science Letters*, 194(1-2): 259-275.
- 728 Snow, J.E. and Reisberg, L., 1995. Os isotopic systematics of the MORB mantle: results from
729 altered abyssal peridotites. *Earth and Planetary Science Letters*, 133(3-4): 411-421.
- 730 Sobolev, A.V., Hofmann, A.W., Kuzmin, D.V. et al., 2007. The amount of recycled crust in sources
731 of mantle-derived melts. *Science*, 316(5823): 412-417.
- 732 Starkey, N., Stuart, F.M., Ellam, R.M., Fitton, J.G., Basu, S. and Larsen, L.M., 2008, in press.
733 Helium isotopes in early Iceland plume picrites: Constraints on the composition of high
734 $^3\text{He}/^4\text{He}$ mantle. *Earth and Planetary Science Letters*, doi:10.1016/j.epsl.2008.10.007.
- 735 Storey, M., Duncan, R.A., Pedersen, A.K., Larsen, L.M. and Larsen, H.C., 1998. $^{40}\text{Ar}/^{39}\text{Ar}$
736 geochronology of the West Greenland Tertiary volcanic province. *Earth and Planetary*
737 *Science Letters*, 160(3-4): 569-586.
- 738 Stracke, A., Bizimis, M. and Salters, V.J.M., 2003. Recycling oceanic crust: Quantitative
739 constraints. *Geochemistry Geophysics Geosystems*, 4: art. no.-8003.
- 740 Stuart, F.M., Lass-Evans, S., Fitton, J.G. and Ellam, R.M., 2003. High $^3\text{He}/^4\text{He}$ ratios in picritic
741 basalts from Baffin Island and the role of a mixed reservoir in mantle plumes. *Nature*,
742 424(6944): 57-59.
- 743 Sun, W., Bennett, V.C., Eggins, S.M., Arculus, R.J. and Perfit, M.R., 2003. Rhenium systematics in
744 submarine MORB and back-arc basin glasses: laser ablation ICP-MS results. *Chemical*
745 *Geology*, 196(1-4): 259-281.
- 746 Taylor, R.N., Thirlwall, M.F., Murton, B.J., Hilton, D.R. and Gee, M.A.M., 1997. Isotopic
747 constraints on the influence of the Icelandic plume. *Earth and Planetary Science Letters*,
748 148(1-2): E1-E8.
- 749 Theriault, R.J., St-Onge, M.R. and Scott, D.J., 2001. Nd isotopic and geochemical signature of the
750 paleoproterozoic Trans-Hudson Orogen, southern Baffin Island, Canada: implications for
751 the evolution of eastern Laurentia. *Precambrian Research*, 108(1-2): 113-138.
- 752 Walker, R.J., Morgan, J.W. and Horan, M.F., 1995. ^{187}Os Enrichment in Some Plumes - Evidence
753 for Core-Mantle Interaction. *Science*, 269(5225): 819-822.

- 754 Walker, R.J., Horan, M.F., Morgan, J.W., Becker, H., Grossman, J.N. and Rubin, A.E., 2002a.
755 Comparative Re-187-Os-187 systematics of chondrites: Implications regarding early solar
756 system processes. *Geochimica et Cosmochimica Acta*, 66(23): 4187-4201.
- 757 Walker, R.J., Prichard, H.M., Ishiwatari, A. and Pimentel, M., 2002b. The osmium isotopic
758 composition of convecting upper mantle deduced from ophiolite chromites. *Geochimica et*
759 *Cosmochimica Acta*, 66(2): 329-345.
- 760 Widom, E. and Shirey, S.B., 1996. Os isotope systematics in the Azores: Implications for mantle
761 plume sources. *Earth and Planetary Science Letters*, 142(3-4): 451-465.
- 762 Widom, E., Hoernle, K.A., Shirey, S.B. and Schmincke, H.U., 1999. Os isotope systematics in the
763 Canary Islands and Madeira: Lithospheric contamination and mantle plume signatures.
764 *Journal of Petrology*, 40(2): 279-296.
- 765 Workman, R.K. and Hart, S.R., 2005. Major and trace element composition of the depleted MORB
766 mantle (DMM). *Earth and Planetary Science Letters*, 231(1-2): 53-72.
- 767 Zindler, A. and Hart, S., 1986. Chemical Geodynamics. *Annual Review of Earth and Planetary*
768 *Sciences*, 14: 493-571.
769
770
771

772 **Figure captions**

773

774 Figure 1. Co-variation of Os and Re with MgO in picrites from West Greenland (WG) and Baffin
775 Island (BI). Other WG, BI and Iceland picrite data from Schaefer et al. (2000), Kent et al. (2004)
776 and Brandon et al. (2007), respectively.

777 Figure 2. Probability density plot for initial $^{187}\text{Os}/^{188}\text{Os}$ in (a) North Atlantic (NA: Baffin Island &
778 West Greenland) picrites from this study and (b) NA and Iceland picrites from the literature (at
779 same scale). Other data: ¹ Schaefer et al. (2000), ² Brandon et al. (2007) and Skovgaard et al.
780 (2001), ³ Kent et al. (2004). NA picrite samples with <0.5 ng/g Os have been omitted due to
781 potential crustal contamination. For comparison, Iceland samples have been corrected to 61 Ma,
782 based on chondritic evolution. A 'bandwidth' uncertainty of 0.001 was applied to the $^{187}\text{Os}/^{188}\text{Os}$
783 ratio of all samples (~0.8% relative uncertainty).

784 Figure 3. Initial $^{187}\text{Os}/^{188}\text{Os}$ (at 61 Ma) plotted against Os concentration. PI, DI and CS are
785 Padloping Island, Durban Island and Cape Searle. An, Nau and Ord are, oldest to youngest,
786 Anaanaa, Naujánguit and Ordlingassoq Members of the Vaigat formation. A lack of co-variation
787 suggests insignificant assimilation of radiogenic ancient crust and/or unradiogenic SCLM. Only the
788 duplicated low Os CS sample has slightly more radiogenic Os than others from Baffin Island,
789 consistent with a minor crustal contribution. Primitive mantle estimate (without uncertainty) from
790 Meisel et al. (2001), abyssal peridotites (AP) from Snow and Reisberg (1995) and Harvey et al.
791 (2006), carbonaceous chondrite (without uncertainty) from Walker et al. (2002a). Other data
792 sources: WG: Schaefer et al. (2000), BI: Kent et al. (2004), Iceland¹: Brandon et al. (2007),
793 Iceland²: Skovgaard et al. (2001).

794 Figure 4. $^{187}\text{Os}/^{188}\text{Os}$ vs. $^{143}\text{Nd}/^{144}\text{Nd}$ (corrected to 61 Ma) for NA picrites in this study (Nd data
795 from Graham et al., 1998; Starkey et al., 2008, in press) and published NA and Iceland picrites

796 (Schaefer et al., 2000; Kent et al., 2004; Brandon et al., 2007). (a) Best estimates for the effects of
797 possible continental crust (CC) assimilation. (b) Mixing between possible mantle components:
798 DMM, PM (primitive mantle), 2 Ga ROC (recycled oceanic crust; gabbro:basalt - 50:50), 2 Ga
799 SROC (ROC:sediment - 95:5, except SROC*: 90:10), and mixing of PM/SROC hybrid component
800 with DMM (superscript numbers refer to the relative proportions in the hybrid). Tick marks
801 represent 10% proportion increments, except where stated. Displayed mantle mixing curves only
802 represent a part of the large possible range due to uncertain parameters and variable mixing
803 proportions. Parameters – see Table 2.

804 Figure 5. Probability density plot for $^{187}\text{Os}/^{188}\text{Os}$ of NA picrites and other direct and indirect
805 indicators of mantle composition. $^{187}\text{Os}/^{188}\text{Os}_{\text{present day}}$ denotes that data, where appropriate, has
806 been corrected for ingrowth since emplacement and then recalculated to a present day mantle
807 composition (assuming chondritic evolution). NA picrites with <0.5 ng/g Os have been omitted due
808 to potential crustal contamination. A ‘bandwidth’ uncertainty of 0.001 was applied to the
809 $^{187}\text{Os}/^{188}\text{Os}$ ratio of all samples ($\sim 0.8\%$ relative uncertainty). Data sources: ¹ This study, Schaefer et
810 al. (2000) and Kent et al. (2004), ² Pearson et al. (2007) and Shi et al. (2007), ³ Walker et al.
811 (2002b; * mean value taken from the authors’ regression using $^{187}\text{Os}/^{188}\text{Os}$ vs. time), ⁴ Roy-
812 Barman and Allegre (1994), Snow and Reisberg (1995), Brandon et al. (2000) and Harvey et al.
813 (2006), ⁵ Gannoun et al. (2007), Global OIB⁶ data from samples with >30 pg/g Os from: Martin,
814 (1991), Hauri and Hart (1993), Reisberg et al. (1993), Martin et al. (1994), Marcantonio et al.
815 (1995), Bennett et al. (1996), Hauri et al. (1996), Widom and Shirey (1996), Widom et al. (1999).
816 EC, OC and CC are enstatite, ordinary and carbonaceous chondrites, respectively (Walker et al.,
817 2002a), PUM is primitive upper mantle (Meisel et al., 2001).

818 Figure 6. He isotope composition against $^{187}\text{Os}/^{188}\text{Os}$ at the time of eruption (61 Ma) for NA
819 picrites (this study, He data from Stuart et al., 2003; Starkey et al., 2008, in press) and recent

820 Icelandic picrites (Brandon et al., 2007). Symbols: see Figure 1. (a) Mixing of isolated depleted
821 3.1 Ga mantle and 2 Ga recycled oceanic crust plus sediment (SROC, ROC:sediment 90:10) and
822 mixing of this hybrid with DMM. Isolated depleted mantle Os and He isotope compositions are
823 based on the He evolution models of ¹ Parman et al. (2007), ² Porcelli and Elliott (2008) and Os
824 isotope evolution assuming a residual [Re] of 0.12 ng/g, similar to an estimate for the DMM (Sun et
825 al., 2003), and [Os] of 3.4 ng/g. As relatively high degree melting is required to generate
826 sufficiently high ³He/⁴He depleted domains (Parman et al., 2005; Porcelli and Elliott, 2008) such a
827 Re content, and therefore also the evolved ¹⁸⁷Os/¹⁸⁸Os, is considered an upper limit. (b) Mixing of
828 primitive mantle, DMM, SROC (ROC:sediment 90:10), and PM/SROC hybrid (superscript
829 numbers refer to the relative proportions in the hybrid). Parameters: see Table 2. Note that there
830 are poor constraints on all He concentrations, and Re-Os abundances in ancient recycled sediment
831 are likely to be extremely heterogeneous. Grey dashed curve in (b) is DMM – PM⁵⁰/SROC⁵⁰
832 mixing modelled with a DMM [He] of 0.269 μcm³(STP)/g used in Brandon et al. (2007).

Table 1

[Click here to download Table: Table 1 a.doc](#)

Table 1. Re-Os isotope and elemental data for North Atlantic picrites (NAP, Baffin Island and Vaigat formation, West Greenland).

	Dig. method	Os ng/g	Re ng/g	Re/Os	¹⁸⁷ Os/ ¹⁸⁸ Os	¹⁸⁷ Os/ ¹⁸⁸ Os _i	¹⁸⁷ Re/ ¹⁸⁸ Os	γOs	MgO wt. %	Ni μg/g	Yb μg/g
Baffin Island											
<i>Padloping Island</i>											
PI-23	CT	1.477	-	-	0.12849	-	-	-	24.51	1127	1.28
PI-24	HPA	1.827	0.173	0.095	0.12775	0.12729	0.457	0.10	26.10	1228	1.27
PI-25	HPA	2.555	0.101	0.040	0.12780	0.12761	0.191	0.35	27.69	1336	1.01
PI-26	HPA	2.028	0.251	0.124	0.12758	0.12698	0.596	-0.15	25.09	1190	1.24
dupl.	HPA	1.927	0.253	0.131	0.12775	0.12711	0.631	-0.04	25.09	1190	1.24
dupl.	CT	1.974	-	-	0.12760	-	-	-	25.09	1190	1.24
PI-27	HPA	1.369	0.336	0.245	0.12896	0.12775	1.168	0.46	23.20	1058	1.30
dupl.	CT	1.483	-	-	0.12849	-	-	-	23.20	1058	1.30
PI-31	HPA	1.762	0.294	0.167	0.12816	0.12734	0.803	0.14	22.64	1027	1.48
PI-37	HPA	3.445	0.120	0.035	0.12692	0.12675	0.168	-0.33	26.57	1206	1.07
PI-43	HPA	2.106	0.295	0.140	0.12777	0.12708	0.674	-0.06	24.58	1081	1.37
PAD-6	HPA	1.084	0.419	0.387	0.12878	0.12689	1.86	-1.06	17.20	647	1.70
<i>Durban Island</i>											
DI-23	CT	2.549	0.097	0.038	0.12751	0.12732	0.182	0.12	24.14	1035	1.32
DI-26	HPA	0.909	0.286	0.315	0.12855	0.12701	1.52	-0.11	15.92	546	1.70
DUR-8	HPA	1.548	0.113	0.073	0.12714	0.12679	0.350	-1.16	22.89	856	1.28
<i>Cape Searle</i>											
CS-7	HPA	0.484	0.506	1.044	0.13356	0.12844	5.03	1.06	20.18	831	1.47
dupl.	HPA	0.435	0.504	1.158	0.13442	0.12874	5.58	1.31	20.18	831	1.47
dupl.	CT	0.471	-	-	0.13369	-	-	-	20.18	831	1.47
W.Greenland											
<i>Anaanaa Member</i>											
400444	CT	1.907	0.259	0.136	0.12812	0.12746	0.655	0.23	20.81	769	1.53
400452	HPA	2.489	0.966	0.388	0.12922	0.12732	1.87	-0.72	21.55	913	1.49
400457	CT	3.879	0.359	0.093	0.12765	0.12720	0.446	0.02	22.65	848	1.40
400492	CT	2.533	1.140	0.450	0.13024	0.12804	2.17	0.70	20.05	801	1.57
408001.233	CT	1.503	0.243	0.162	0.12824	0.12746	0.779	0.22	17.99	751	1.45
<i>Naujanguit Member</i>											
113210	CT	3.119	0.206	0.066	0.12725	0.12693	0.318	-0.19	20.88	920	
264217	CT	2.786	0.472	0.169	0.12772	0.12689	0.816	-0.21	21.97	949	1.50
332771	CT	1.553	0.425	0.274	0.12837	0.12704	1.32	-0.10	20.09	824	1.57
362149	CT	2.813	0.291	0.103	0.12814	0.12759	0.550	0.33	23.45	1329	1.33
400485	HPA	4.024	0.316	0.079	0.12713	0.12674	0.378	-1.19	27.02	1184	1.17
<i>Ordlingassoq Member</i>											
113333	CT	2.256	0.063	0.028	0.12955	0.12942	0.134	1.77	20.53	935	
138228	CT	1.524	0.330	0.216	0.13321	0.13216	1.04	3.92	17.17	850	
332788	CT	2.034	0.180	0.089	0.13120	0.13094	0.427	2.97	25.62	1306	1.13
332828	CT	2.680	0.367	0.137	0.13060	0.12994	0.660	2.17	22.23	1098	1.35
332901	HPA	1.727	0.071	0.041	0.13123	0.13103	0.198	2.15	24.60	1098	1.22
354754	HPA	2.198	0.179	0.082	0.13254	0.13214	0.393	3.02	20.74	810	1.45
400230	HPA	2.768	0.335	0.121	0.13235	0.13175	0.584	2.72	21.77	935	1.43

Notes:

Reference materials analysed during the period of analysis (using HPA digestion) have been published previously in Dale et al. (2008) and Dale et al. (in review)

$^{187}\text{Os}/^{188}\text{Os}_i$ – Os isotope composition corrected for ingrowth of ^{187}Os since the time of emplacement (61 Ma).

γOs – deviation of $^{187}\text{Os}/^{188}\text{Os}_i$ from the chondrite evolution curve: $((^{187}\text{Os}/^{188}\text{Os}_i / ^{187}\text{Os}/^{188}\text{Os}_{\text{chondrite}}) - 1) * 100$.

Digestion method: HPA – high-pressure asher, CT – Carius tube, both digestions in inverse aqua regia.

Sample mass digested approx. 1g in all cases.

Figure 1

[Click here to download Figure: Fig 1 - MgO vs Os-Re.eps](#)

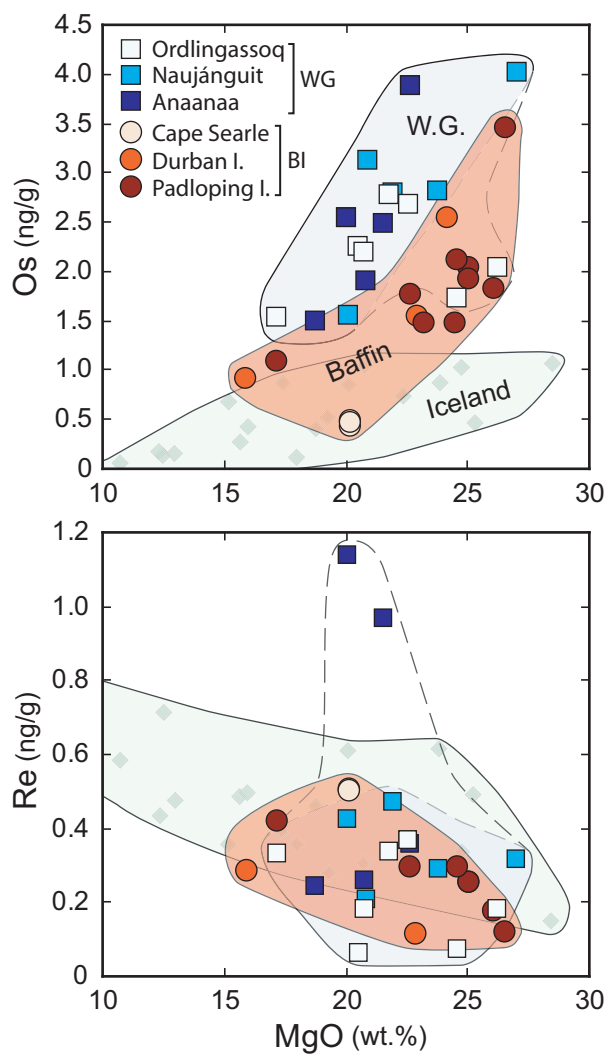


Figure 2

[Click here to download Figure: Fig 2 - New Os prob density new.eps](#)

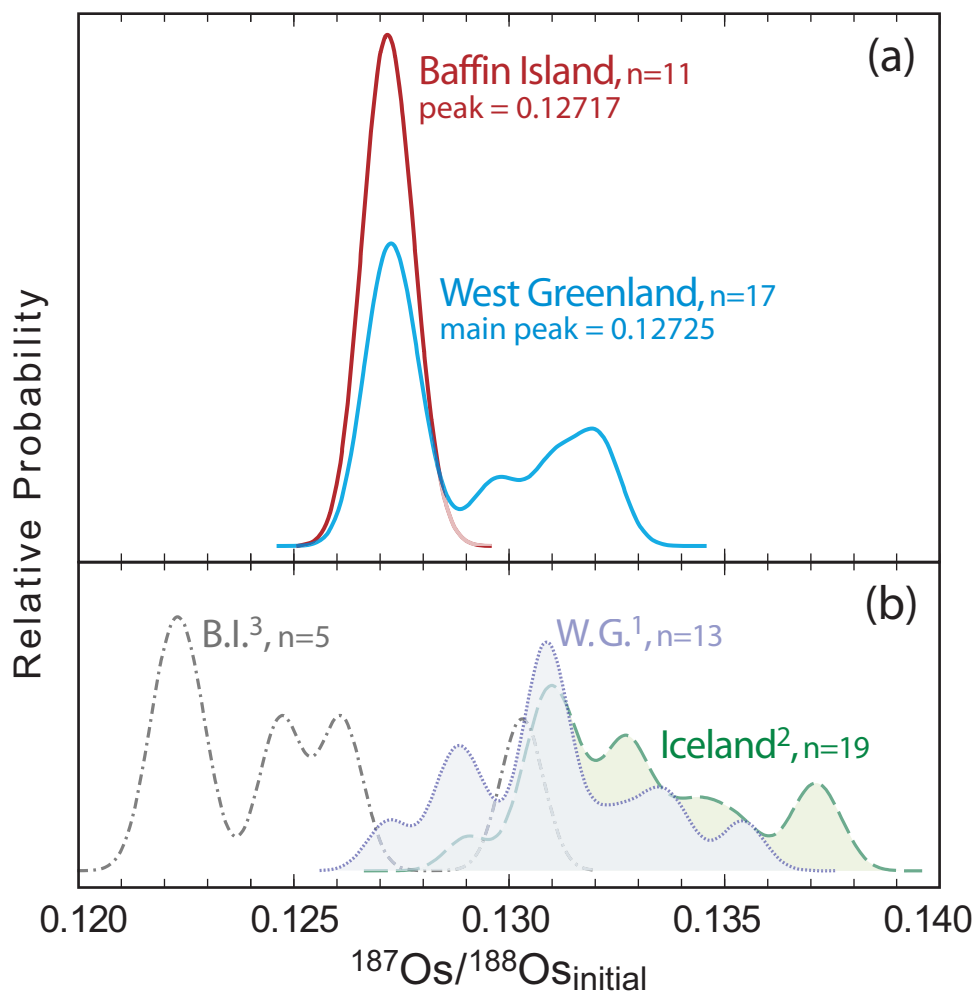


Figure 3
[Click here to download Figure: Fig 3 - Os v 187-188Os.eps](#)

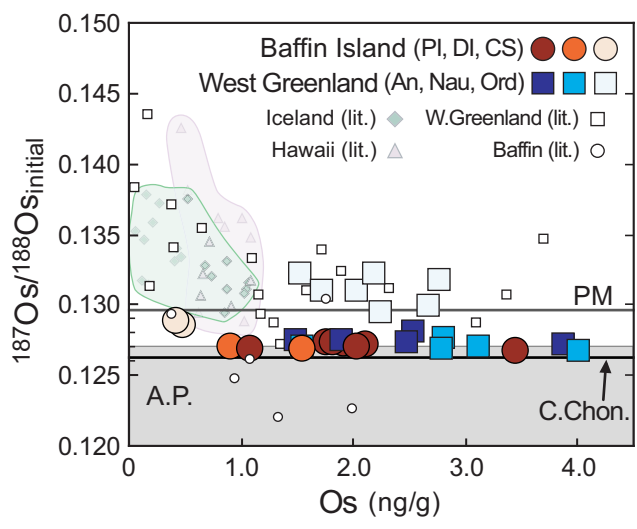


Figure 4

[Click here to download Figure: Fig 4 - 187-188Os v Nd.eps](#)

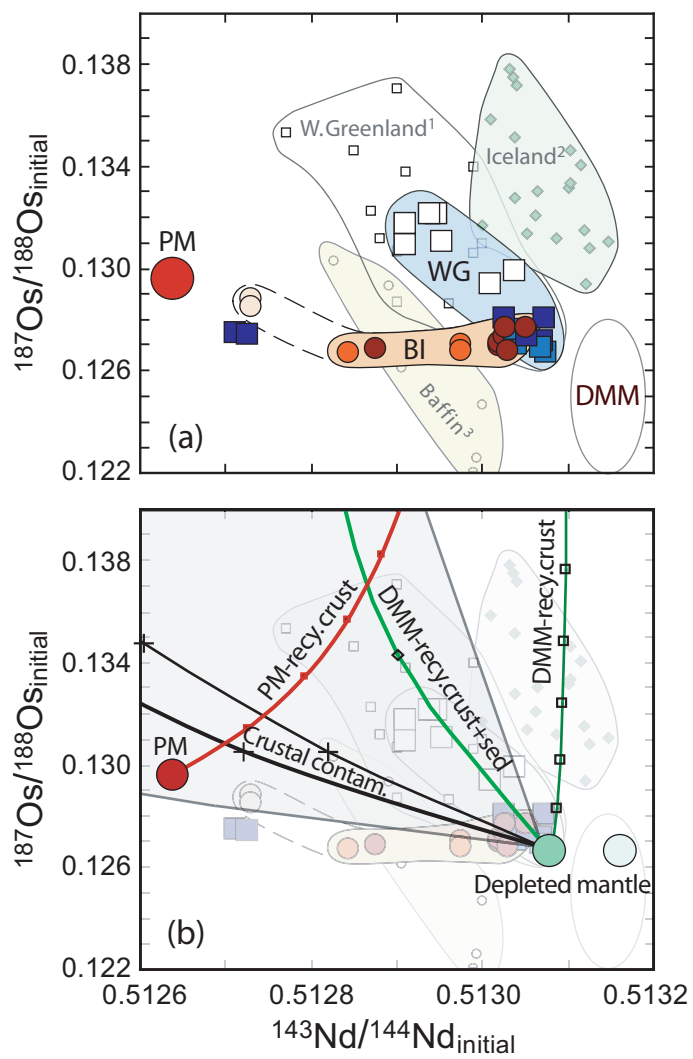


Figure 5

[Click here to download Figure: Fig 5 - New Os prob density new.eps](#)

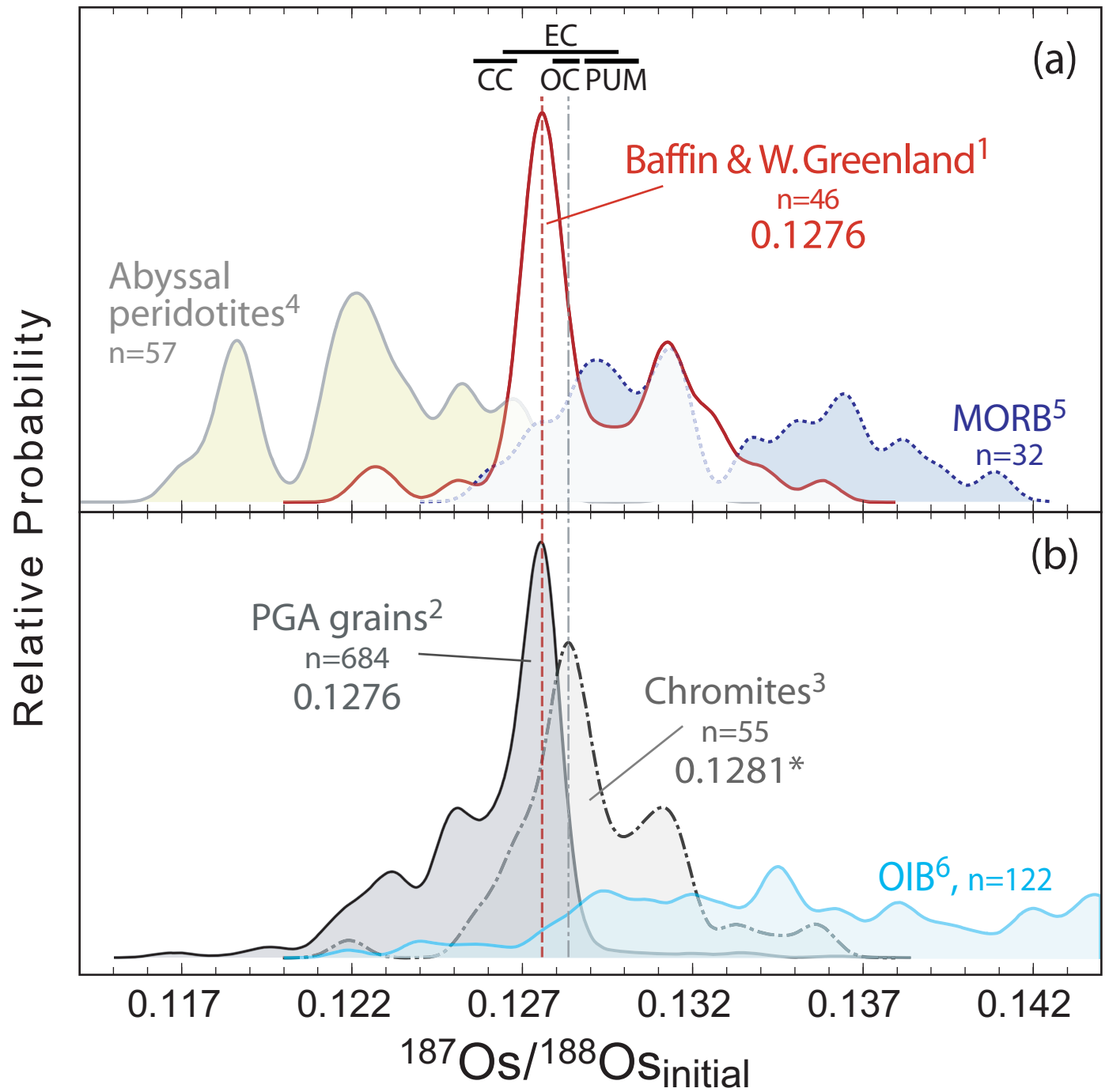


Figure 6

[Click here to download Figure: Fig 6 - 3-4He v 187-188Os & Os PDF.eps](#)

